

## Frequency-resolved photoelectron spectra of two-photon ionization of He by an attosecond pulse train

E P Benis<sup>1</sup>, P Tzallas<sup>1</sup>, L A A Nikolopoulos<sup>2</sup>, M Kovačev<sup>1</sup>,  
C Kalpouzos<sup>1</sup>, D Charalambidis<sup>1</sup> and G D Tsakiris<sup>3</sup>

<sup>1</sup> Foundation for Research and Technology—Hellas,  
Institute of Electronic Structure and Laser, PO Box 1527,  
GR-71110 Heraklion (Crete), Greece

<sup>2</sup> Department of Telecommunication Sciences and Technology,  
University of Peloponnisos, GR-22100 Tripoli, Greece

<sup>3</sup> Max-Planck-Institut für Quantenoptik, D-85748 Garching, Germany  
E-mail: [benis@iesl.forth.gr](mailto:benis@iesl.forth.gr)

*New Journal of Physics* **8** (2006) 92

Received 20 February 2006

Published 9 June 2006

Online at <http://www.njp.org/>

doi:10.1088/1367-2630/8/6/092

**Abstract.** We present measured and calculated energy-resolved photoelectron spectra obtained through two-photon ionization of He induced by a superposition from the 9th to the 15th harmonic of a Ti:Sapph laser forming an attosecond (asec) pulse train. The reported measured spectra are a decisive step towards frequency-resolved two-XUV-photon ionization-based second-order autocorrelation (AC) of asec pulse trains, and thus towards a complete reconstruction of asec pulses.

Since the dawn of the experimental demonstration of attosecond (asec) pulse trains [1]–[4] or asec isolated pulses [5], their rigorous characterization has been a most challenging problem. Asec pulses pave the way to the ever higher temporal resolution of electronic dynamics in matter [6]. Thus, the complete characterization of such pulses is an indispensable prerequisite for the detailed understanding of the dynamics in ultra-fast physical processes.

Although at visible and infrared (IR) wavelengths femtosecond (fs) pulses are routinely characterized by standard techniques based on a nonlinear effect induced exclusively by the radiation to be characterized, such as nonlinear AC, frequency-resolved optical gating (FROG) [7] and spectral phase interferometry for direct electric-field reconstruction (SPIDER) [8], it is nontrivial to extend the above techniques to the XUV region, due to the lack of XUV beam

splitters and the difficulty of inducing nonlinear processes in this spectral region. These obstacles have forced the use of advanced cross-correlation techniques, utilizing the fundamental laser frequency, as diagnostic instruments of asec pulses [2, 3, 5]. Cross-correlation approaches served as a valuable tool in the early stage of attoscience. However, continuous advances in laser technology allow more efficient XUV generation, and thus the use of more direct characterization methods [4]. Furthermore, spatiotemporal effects complicate the extraction of asec pulse durations, in approaches based on the measurement of ‘averaged’ harmonic phases [9]–[11]. So far the first direct measurement of the spatiotemporal averaged duration of the individual pulses of an asec pulse train were based on a second-order AC technique [4]. An extension of this measurement to a FROG-like approach in the XUV spectral region will allow for a detailed temporal reconstruction of asec pulses. This requires a frequency-resolved two-XUV-photon ionization measurement, provided by the energy-resolved photoelectron (PE) spectroscopy of the two-photon ionization.

Recently, successful attempts towards extending the well-established standards of fs metrology to XUV pulses have been reported for individual harmonics. Thus, a second-order AC-based frequency-resolved two-XUV-photon gating measurement of individual harmonic pulses has been demonstrated [12], while the observation of single-colour two-XUV-photon above threshold ionization (ATI) [13] and two-photon double ionization [14] open up promising perspectives for second-order AC-based characterization techniques for a wide XUV spectral range. The first measurement of an individual harmonic combining a second-order AC technique with two-XUV-photon ATI has already been reported [15].

In this paper, we report the first PE spectrum of two-photon ionization of He by an asec pulse train [4]. An energy-resolved PE spectrum resulting from He ionization by any two-photon combination of the 9th, 11th, 13th and 15th harmonics of a Ti:Sapph laser at 800 nm has been recorded. Our result is the continuation of the previous work on TPI by a coherent superposition of harmonics [16] and on the second-order AC measurements [4, 17], that constitutes a decisive step towards frequency-resolved two-XUV-photon ionization gating, i.e. FROG-like measurement in the XUV spectral region. It is worth noting that the present work is highly pertinent to the diagnostics and applications of other XUV radiation sources and in particular to the upcoming advanced free electron laser (FEL)-based sources, the high brightness of which strongly supports nonlinear processes at short wavelengths. In particular, considering the difficulties faced by the synchronization between laser and FEL pulses, due to the inherent large FEL jitter, approaches utilizing solely the radiation to be characterized, like second-order AC or FROG, are highly desirable. It is needless to mention that mapping out the significant phase variations of the FEL radiation requires appropriately high resolution in the PE spectra. Given the anticipated high FEL photon fluxes, the PE spectral resolution can be as good as 0.1% using contemporary spectrometers.

The experiment was performed utilizing a 10 Hz repetition rate Ti:Sapph laser system delivering 50 fs pulses with energy up to  $150 \text{ mJ pulse}^{-1}$  and a carrier wavelength of 800 nm. The experimental setup is similar to that in [4] and shown in figure 1. An annular laser beam of 2 cm outer diameter and  $15 \text{ mJ pulse}^{-1}$  energy was focused by a 3.5 m focal length lens on to the pulsed Xe gas jet where the harmonics were generated. Two pinholes with diameters of 1 and 3 mm were located at 15 and 40 cm downstream respectively, forming a differentially pumped chamber to isolate the harmonic generation region from the detection region. As the XUV+IR beam was spatially expanded, a second aperture placed 2 m after the Xe gas jet blocked the annular part of the IR beam. A  $0.2 \mu\text{m}$  thickness Sn filter located after the aperture served for

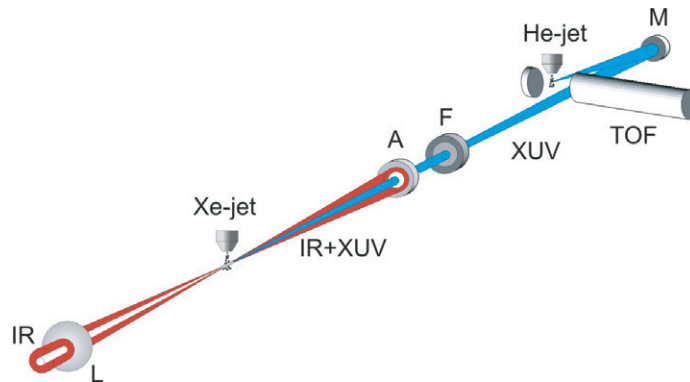


**Figure 1.** The experimental setup. L: 3 m focal length lens, A: aperture, F: Sn filter, M: spherical mirror.

selecting the 9th–15th harmonics and further blocking the IR radiation. The XUV beam was then reflected by a tungsten spherical mirror of 5 cm focal length (located 3 m downstream from the Xe gas jet) at nearly normal incidence ( $1.7^\circ$ ), to be focused on to the pulsed He gas jet. The small deviation from the normal incidence is in order to bring the focus of XUV beam as close as possible to the jet orifice. The ionization products (selectively electrons or ions) were detected with a  $\mu$ -metal shielded time-of-flight (TOF) spectrometer.

The spectral intensity distribution of the harmonics was obtained by the PE energy spectra of Xe and Ar rare gases. The single-photon ionization of Ar has a practically flat cross-section for the harmonics of interest here [19]. However, the 9th harmonic amplitude was obtained from the Xe PE spectrum in comparison to Ar, since the photon energy of the 9th harmonic is not sufficient to ionize Ar. The single-photon ionization of Xe spans a factor of two in the cross-section of the harmonics of interest here [19], and this fact was taken into account. Thus, the relative harmonic field amplitudes were obtained to be  $9 : 11 : 13 : 15 \rightarrow 0.35 : 0.55 : 1 : 0.69$ . The single-photon ionization electron spectra of Ar and Xe were used also for the energy calibration of the TOF spectrometer.

For the above experimental conditions, taking into account the XUV conversion efficiency factor of the order of  $10^{-5}$  into the first Xe gas jet [20], the 25% transmission of the Sn filter, and the 35% reflectivity of the tungsten mirror, the total harmonic energy into the interaction region was estimated to be about 25 nJ. Based on the findings of similar experimental conditions about the harmonic angular divergence, and the pulse duration for each harmonic,  $\tau_q \cong \tau_L / \sqrt{p}$ , where  $\tau_L$  is the laser pulse duration and  $p = 6$  the effective order of nonlinearity for the harmonic generation [17, 21], the XUV intensity at the interaction region was estimated up to the order of  $10^{12} \text{ W cm}^{-2}$ .

In order to establish the nonlinear TPI process, the XUV power dependence of the  $\text{He}^+$  yield was studied as a function of the total XUV intensity [16]. In figure 2, the  $\text{He}^+$  (two-photon ionization) and  $\text{Ar}^+$  (single-photon ionization) ion yields are plotted as a function of the XUV intensity, which was controlled through the Xe gas pressure by varying the delay time between the opening of the nozzle and the laser pulse. The slopes were found to be  $1.9 \pm 0.2$  and  $1.0 \pm 0.1$  for  $\text{He}^+$  and  $\text{Ar}^+$  respectively, in agreement with the intensity dependence of the two ionization processes. Measured electron signals were, by a factor of 20, weaker than ionic ones.

The observed PE energy spectrum is shown in figure 3(a), where the harmonic combination channels  $9 + 13 \oplus 11 + 11$  and  $9 + 15 \oplus 11 + 13$  corresponding to PE energies 9.5 and 12.6 eV

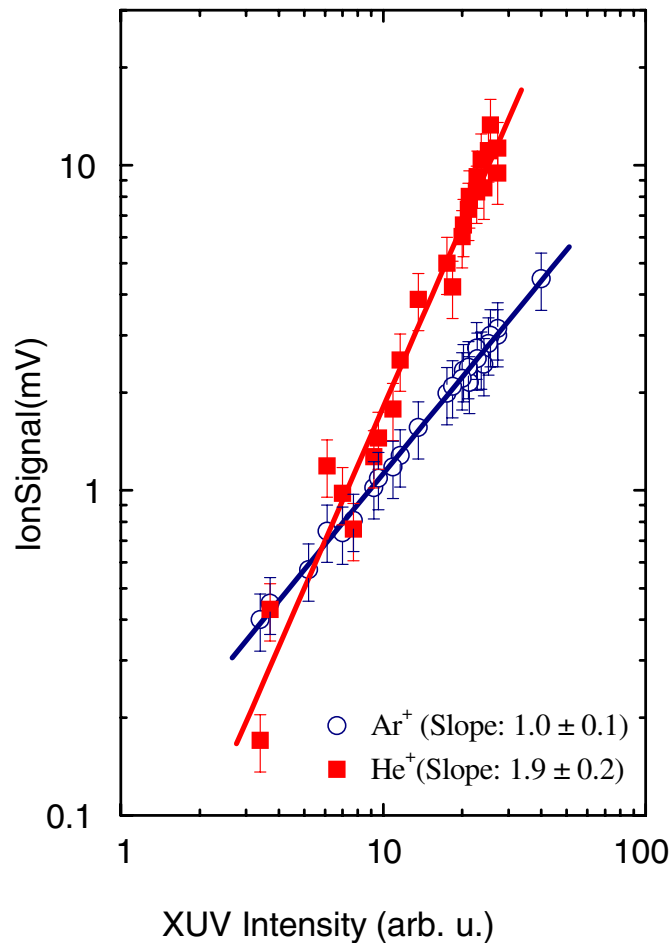


**Figure 2.** He<sup>+</sup> and Ar<sup>+</sup> ion yields obtained as a function of the XUV intensity. The slope of  $1.9 \pm 0.2$  for He<sup>+</sup> ascertains the nonlinear two-photon ionization process for He in contrast to the linear single-photon ionization process for Ar ensured by the slope of  $1.0 \pm 0.1$ . Ar<sup>+</sup> ion yield has been divided by a factor of 10.

respectively, are clearly observed. There is also indication about the observation of two more channels, the  $9 + 11$  and  $11 + 15 \oplus 13 + 13$ , which will be commented on later. In the shown spectrum, the continuous background originating from surface PEs has been subtracted. The peak height signals were found to be well within the experimentally expected values. The two additional peaks at energies 4.4 and 7.5 eV correspond to the single-photon ionization of Ar by the 13th and 15th harmonics respectively. Ar contaminants in the gas jet are present in the PE spectra as the single-photon ionization probability is orders of magnitude larger than the two-photon non-resonant ionization probability, and were used for the TOF self-calibration. Note that the acquisition time for a ‘useful’ PE spectrum reads a few minutes.

*Ab initio* calculations based on a two-electron basis expansion technique have been utilized in numerically solving the six-dimensional (three for each electron) He time-dependent Schrödinger equation (TDSE)  $i\partial_t\psi(t) = [H_0 + D(t)]\psi(t)$  (atomic units).  $H_0$  is the field-free Hamiltonian,  $D(t) = -\vec{E}(t) \cdot \vec{r}$  the electric-dipole interaction with the field  $\vec{E}(t)$  of the

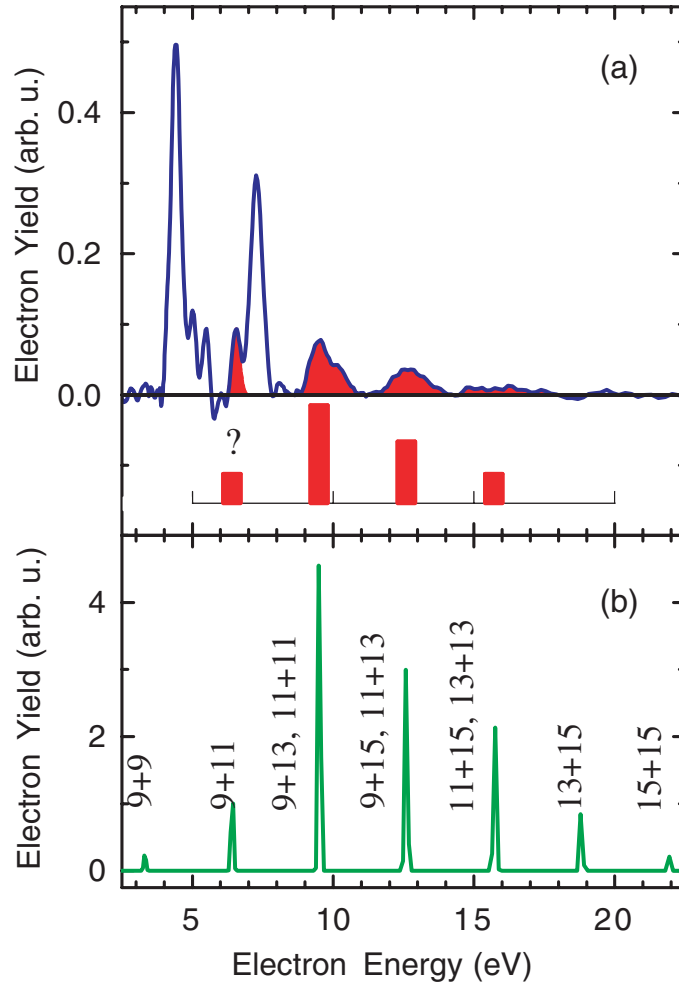


**Figure 3.** (a) The measured energy-resolved PE spectrum of two-XUV-photon ionization of He is depicted by the shaded areas. The two peaks at energies 4.4 and 7.5 eV correspond to the single-photon ionization of Ar by the 13th and 15th harmonics respectively. (b) Theoretical energy PE spectrum obtained by solving the He TDSE in the XUV field formed by the superposition from the 9th to the 15th harmonic of a Ti:Sapph laser. Harmonic phases were obtained by the three-step rescattering model for a laser intensity of  $7 \times 10^{13} \text{ W cm}^{-2}$ .

harmonics superposition and  $\vec{r} = \vec{r}_1 + \vec{r}_2$  the position vector of the two He electrons. The field of the harmonics' superposition was assumed linearly polarized along the TOF axis and realized as  $E(t) = \sum_{q=9,11,13,15} E_i f(t) \sin(q\omega t + \varphi_q)$ , where  $\omega$  is the fundamental frequency,  $q$  the harmonic order,  $\varphi_q$  the phase of the  $q$ th harmonic,  $E_i$  the harmonic amplitudes and  $f(t) = \exp[-2 \ln 2(t/\tau)^2]$  is the Gaussian pulse envelope with full-width at half-maximum (FWHM)  $\tau = 20$  fs. An intensity of  $10^{12} \text{ W cm}^{-2}$  was assumed. Details on the theoretical calculations can be found elsewhere [16, 18, 22]. In figure 3(b) the theoretically calculated energy-resolved PE spectrum for the two-photon ionization of He with amplitudes corresponding to the experimentally determined values, and phases  $\varphi_q$  resulting from the three-step rescattering model for a laser intensity of  $7 \times 10^{13} \text{ W cm}^{-2}$  are shown [10].

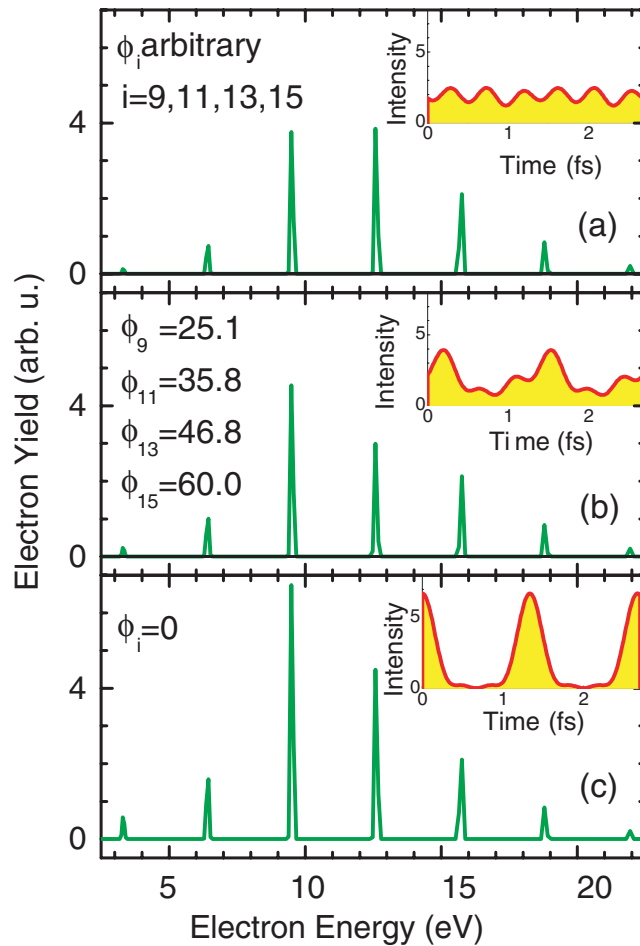


**Figure 4.** Calculated energy-resolved PE spectra for three different sets of harmonic phases  $\varphi_q$  are compared: (a) arbitrary phases resulting in a structureless pulse, (b) phases resulting from the three-step rescattering model, and (c) all phases are set equal to zero. The insets depict the corresponding pulses.

Based on the above calculations and taking into account the weak electron signals expected experimentally, the strongest detectable channels are the  $9 + 13 \oplus 11 + 11$  and  $9 + 15 \oplus 11 + 13$ , and they were clearly observed in the experiment. As was earlier stated there is also an indication about the observation of channels  $9 + 11$  and  $11 + 15 \oplus 13 + 13$ . It is instructive to notice here that in TOF spectrometers, the absolute width of a peak in the energy spectra broadens at larger energies, as it is seen in figure 3(a). Taking this into account and the fact that the theoretically expected signal is about one-third of the strongest channel, the indication of a broad small peak at the energy of 15.7 eV is rather convincing. The same reasoning may well be applied to the  $9 + 11$  channel although with less confidence since the signal is one-fifth of the strongest channel. The ratio of the areas of the observed channels was extracted and shown in the inset of figure 3(a) in comparison to the corresponding channels theoretically calculated. As can be seen there is good agreement between the measured and calculated spectra.

In figure 4, the calculated PE energy spectra for three different sets of harmonic phases  $\varphi_q$  are compared. In figure 4(a), arbitrary phases have been used resulting in a structureless

pulse. In figure 4(b), phases resulting from the three-step rescattering model have been used, while in figure 4(c) all phases are set equal to zero, i.e. Fourier transform limited (FTL) pulses. The insets depict the corresponding pulses. As can be seen, the PE spectral distribution depends on the temporal characteristics of the ionizing radiation. As temporal localization becomes stronger, the electron yield increases as a result of the higher intensity that induces the nonlinear ionization. The relative peak heights depend on the ionizing pulse shape as well. From this result, it is apparent that the spectral PE intensity distribution itself compared to calculated spectra gives partial information about the harmonic phases. However, at the low signal level of the present experiment such a comparison would not be reliable enough.

In conclusion, the first energy-resolved PE spectrum resulting from He two-photon ionization induced by a superposition from the 9th to the 15th harmonic of a Ti:Sapph laser forming an asec pulse train has been reported. *Ab initio* calculations are in reasonable agreement with the data regarding the ratio of the observed PE peaks. This is a vital step towards second-order AC FROG-like measurements of asec pulse trains, and thus towards their complete reconstruction. An increased PE energy resolution and signal would improve the accuracy of the approach, towards which work is in progress.

After submission of this paper, a related work has been reported in [23].

## Acknowledgments

This work was supported in part by the European Community's Human Potential Programme under contract MRTN-CT-2003-505138 (XTRA), MIRG-CT-2004-506583 (CHARA), MTKD-CT-2004-517145 X-HOMES, and the Ultraviolet Laser Facility (ULF) operating at FORTH-IESL (contract no HPRI-CT-2001-00139). MK acknowledges support from the AvH Stiftung.

## References

- [1] Papadogiannis N A, Witzel B, Kalpouzos C and Charalambidis D 1999 *Phys. Rev. Lett.* **83** 4289
- [2] Paul P M, Toma E S, Bregger P, Mullot G, Augé F, Balcou Ph, Muller H G and P 2001 *Science* **292** 1689
- [3] Mairesse Y *et al* 2003 *Science* **302** 1540
- [4] Tzallas P, Charalambidis D, Papadogiannis N A, Witte K and Tsakiris G 2003 *Nature (London)* **426** 267
- [5] Hentschel M *et al* 2001 *Nature (London)* **414** 509  
Kienberger R *et al* 2002 *Science* **297** 1144  
Kienberger R *et al* 2004 *Nature (London)* **427** 817
- [6] Drescher M *et al* 2002 *Nature (London)* **419** 803  
Niikura H, Legarè F, Hasbani R, Bandrauk A D, Ivanov M Y, Villeneuve D M and Corkum P B 2002 *Nature (London)* **417** 917  
Niikura H, Legarè F, Hasbani R, Ivanov M Y, Villeneuve D M and Corkum P B 2003 *Nature (London)* **421** 826  
Itatani J, Levesque J, Zeidler D, Niikura H, Pèpin H, Kieffer J C, Corkum P B and Villeneuve D M 2004 *Nature (London)* **432** 867  
Johnsson P *et al* 2005 *Phys. Rev. Lett.* **95** 013001
- [7] Trebino R, DeLong K W, Fittinghoff D N, Sweetser J N, Krumbügel M A and Richman B 1997 *Rev. Sci. Instrum.* **68** 3277
- [8] Iaconis C and Walmsley I A 1999 *IEEE J. Quantum Electron.* **35** 501
- [9] Kazamias S and Balcou Ph 2004 *Phys. Rev. A* **69** 063416

- [10] Nikolopoulos L A A, Benis E P, Tzallas P, Charalambidis D, Witte K and Tsakiris G D 2005 *Phys. Rev. Lett.* **94** 113905
- [11] Mairrese Y and Quere F 2005 *Phys. Rev. A* **71** 011401
- [12] Sekikawa T, Katsura T, Miura S and Watanabe S 2003 *Phys. Rev. Lett.* **88** 193902
- [13] Miyamoto N, Kamei M, Yoshitomi D, Sekikawa T, Nakatjima T and Watanabe S 2003 *Phys. Rev. Lett.* **93** 083903
- [14] Nabekawa Y, Hasegawa H, Takahashi E J and Midorikawa K 2005 *Phys. Rev. Lett.* **94** 043001
- [15] Sekikawa T, Kosuge A, Kanai T and Watanabe S 2004 *Nature (London)* **432** 605
- [16] Papadogiannis N A, Nikolopoulos L A A, Charalambidis D, Tsakiris G D, Tzallas P and Witte K 2003 *Phys. Rev. Lett.* **90** 133902
- [17] Tzallas P, Charalambidis D, Papadogiannis N A, Witte K and Tsakiris G D 2005 *J. Mod. Opt.* **52** 321
- [18] Nikolopoulos L A A and Lambropoulos P 2001 *J. Phys. B: At. Mol. Opt. Phys.* **34** 545
- [19] Swanson J R and Armstrong L Jr 1977 *Phys. Rev. A* **15** 661
- [20] Hergot J F, Kovačev M, Merdji H, Hubert C, Mairesse Y, Jean E, Breger P, Agostini P, Carré B and Salières P 2002 *Phys. Rev. A* **66** 021801(R)
- [21] L'Huillier A, Balcou P, Candel S, Schafer K J and Kulander K C 1992 *Phys. Rev. A* **46** 2778
- [22] Lambropoulos P, Maragakis P and Zhang J 1998 *Phys. Rep.* **305** 203
- [23] Nabekawa Y, Shimizu T, Okino T, Furusawa K, Hasegawa H, Yamanouchi K and Midorikawa K 2006 *Phys. Rev. Lett.* **96** 083901